Enhanced Lithium Absorption in Single-Walled Carbon Nanotubes by Boron Doping

Zhen Zhou,*,†,‡ Xueping Gao,‡ Jie Yan,‡ Deying Song,‡ and Masahiko Morinaga†

Department of Materials Science and Engineering, Graduate School of Engineering, Nagoya University, Furo-cho, Chikusa-ku, Nagoya 464-8603, Japan, and Institute of New Energy Material Chemistry, Nankai University, Tianjin 300071, China

Received: March 1, 2004; In Final Form: April 9, 2004

The lithium absorption energies and electronic structures of the boron-doped single-walled carbon nanotubes (SWCNT) were investigated using the first-principles calculations. The lithium absorption energies in the B-doped SWCNTs are large negative values, compared with those in the pure SWCNT, whether Li is absorbed at inner sites or at outer sites of the tube walls. The B doping forms an electron-deficient structure in SWCNT, which can effectively accept the electrons from the absorbed Li and stabilize the Li absorption on the tube wall. The calculation results suggest that enhanced Li absorption capability in the B-doped SWCNT should be expected.

1. Introduction

Carbon nanotubes have the promising applications in hydrogen storage[1,2] and Li ion secondary batteries.[3−7] In Li ion batteries, graphitic carbon materials are used instead of metallic Li electrodes for the consideration of safety and cycle efficiency.[8] However, the use of graphite as a host material leads to a specific capacity reduction, so carbon nanotubes are expected to exhibit superior Li absorption capabilities. Unfortunately, experimental results were somewhat disappointing for Li intercalation into carbon nanotube systems on both multi-walled[9] and single-walled[10,11] nanotubes, showing only 25% higher reversible capacity of Li than graphite. To get an understanding of how to improve the Li absorption in carbon nanotube systems, several important issues need to be addressed. For example, the diffusion mechanisms and the effects of the defects are important.[12] On the other hand, introduction of some impurities into carbon nanotubes should also be explored.

In this investigation, the (5, 5) single-walled carbon nanotube (SWCNT) was used as a model, and the doping effects of boron were investigated using the first-principles calculations. The energetics and electronic structures were evaluated in SWCNT supercells, and the emphasis is laid on the B-doping effects on the Li absorption, and the Li absorption capability could be predicted through such calculations, which proved very helpful in the investigations of Li intercalation in the cathode materials of Li batteries.[13]

2. Computational Details

The first-principles calculations based on the density function theory (DFT) were performed in this investigation with the generalized gradient approximation (GGA) by Perdew et al.[14] The implementation of DFT employed here combines a plane-wave basis set with the total energy pseudopotential method, as is embodied in the CASTEP code.[15] In the present calculations, ultrasoft pseudopotentials proposed by Vanderbit[16] were employed. The calculations were carried out using a periodically repeating tetragonal supercell with lattice constants a_{sc}, b_{sc}, and c_{sc}. The lattice constants, a_{sc} and b_{sc}, are chosen such that the interaction between nearest-neighbor tubes is negligible (the minimum C−C distance between two nearest neighbor tubes is taken as about 10 Å). The lattice constant along the tube axis, c_{sc}, is taken to be equal to twice that of the one-dimensional lattice parameter c of the tube.[17] An energy cutoff of 400 eV for the plane waves was used in all the calculations, and k-point sampling was done only along the tube axis. The Monkhorst−Pack special k-point scheme is used with six k points. The positions of all C atoms, the doped B atoms, and absorbed Li atoms were fully relaxed. The optimization procedure was truncated when the energy change per atom was less than 1×10^{-5} eV, the root mean square (RMS) of the forces was less than 0.03 eV/Å, and the RMS displacement of atoms during the geometry optimization was less than 1×10^{-3} Å. The formation energy of the doped B in SWCNT was calculated using the total energies of the supercells. The formation energy, E_{form}, is defined as follows

$$E_{form} = E_{tot}(\text{doped}) - E_{tot}(\text{perfect}) + \mu_C - \mu_B \qquad (1)$$

where E_{tot}(doped) is the GGA total energy for the supercell in which a B atom is substituted for a C atom and E_{tot}(perfect) is the total energy for a perfect SWCNT supercell. μ_C is the chemical potential of carbon, and μ_B is the chemical potential of the doped B atom, obtained by calculating the total energy per atom for the bulk B.

The Li absorption energy is defined as the change in the total energy due to the Li absorption, which is a measure of the tendency for Li absorption to occur in SWCNT, and is calculated using the expression

$$E_{absorption} = E_{tot}(\text{Li−host}) - E_{tot}(\text{host}) - \mu_{Li} \qquad (2)$$

in terms of the GGA total energies of the fully optimized pure SWCNT or boron-doped SWCNT hosts (E_{tot}(host)) and Li-absorbed hosts (E_{tot}(Li−host)). Similarly, μ_{Li} was obtained by calculating the total energy per atom for Li metal. By definition, $E_{absorption} < 0$ in eq 2 corresponds to a stable and exothermic

* To whom correspondence may be addressed. Tel.: +81-52-789-4203. Fax: +81-52-789-3233. E-mail: shushin@silky.numse.nagoya-u.ac.jp.
† Nagoya University.
‡ Nankai University.

10.1021/jp049086z CCC: $27.50
Published on Web 05/27/2004

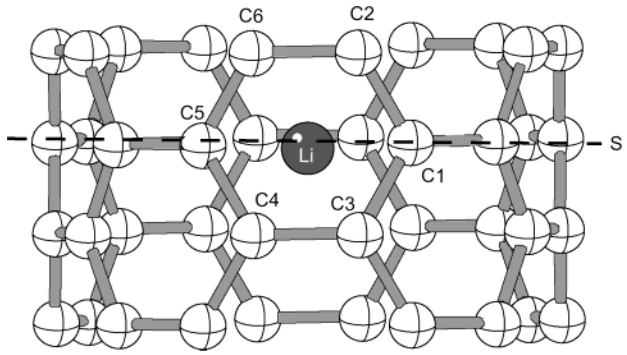

Figure 1. Side view of the model of Li-absorbed pure (5, 5) SWCNT. In the B-doped SWCNT, the carbon atom named as C1 or C3 is substituted with a B atom, respectively. The Li absorption energies were calculated for two possible sites, i.e., inner and outer sites. The slash S indicates the cross section including the absorbed Li and the B atom substituted for the C1 atom.

TABLE 1: Li Absorption Energies for the Pure and B-Doped (5, 5) SWCNTs

Li absorption site	Li absorption energy/eV		
	pure SWCNT	B_{C1}-doped SWCNT	B_{C3}-doped SWCNT
inner	0.34	−0.73	−0.72
outer	0.41	−0.72	−0.77

chemical absorption. If $E_{absorption} > 0$, it is an endothermic process. The model used in the investigation is shown in Figure 1. In the B-doped SWCNT, the carbon atom named as C1 or C3 is substituted with a B atom, respectively. Hereafter they are called B_{C1}-doped SWCNT and B_{C3}-doped SWCNT, respectively. The Li absorption energies were calculated for two possible sites, i.e., inner and outer sites. Test calculations were conducted for the Li absorption in graphite, and the calculated $E_{absorption}$ is about −0.21 eV, which is reasonable compared with the experimental and calculated results, −0.145 eV.[18,19]

3. Results and Discussion

3.1. Lithium Absorption Energies. The absorption energies for the pure and B-doped (5, 5) SWCNT are listed in Table 1. In the pure SWCNT, the absorption energies for Li absorbed both at inner and outer sites are positive values, indicating that Li absorption in pure (5, 5) SWCNT is not favorable energetically, according to the definition of the Li absorption energy in eq 2. The Li absorption energies for the B-doped SWCNTs are much lower than those of the pure SWCNT both at inner and outer sites; moreover, they are quite negative values. This is the interesting point due to the B doping in SWCNT. The B-doped SWCNT will provide more energetically favorable sites for Li absorption. The high absorption energy means strong interaction between the absorbed Li and the host, which will be discussed in the following in detail. The strong interaction between the absorbed Li and the host may effectively compensate the repulsion among the absorbed Li ions and stabilize the structure of the Li-absorbed host, when more Li ions are considered to be absorbed. Therefore, the B doping may make high-density storage of Li available in SWCNT. Surely, the lithium absorption is a kinetic process; the lithium diffusion path should also be considered in order to fully understand the Li absorption process.[20] The diffusion barriers for Li motion are quite low inside the nanotubes themselves,[13] so the key problem is the entry channel for Li into SWCNT. Theoretical investigations showed that the entry of Li ions into pristine tubes through the tube walls is forbidden; however, Li can enter the tubes through topological defects and open-ended tops. The B doping might decrease the energy barrier to a certain degree when Li diffuses through the tube walls, but it is still needed some more calculations to evaluate whether the decrease in the energy barrier can make the entry through the tube walls possible. This part of the investigation is not included in this paper.

3.2. Electronic Structures. The effects of B doping on the Li absorption in SWCNT are strongly related to the electronic structure. The band structures and total density of states (DOS) are shown in Figure 2 for the pure and B-doped (5, 5) SWCNT.

In Figure 2, the B-doping forms an acceptor-like level above the valance band maximum. Also, the contour plots for the charge density in the pure and B-doped SWCNT are shown in Figure 3, which can clearly describe the changes in the electronic structures due to the B doping. It can clearly be seen from Figure 3 that a localized electron-deficient structure forms in SWCNT due to the B doping. When the chemical bonding around the absorbed Li is carefully checked, it can be found from Table 2 that, when Li is absorbed at inner sites, the Li−B distance in the B_{C1}-doped SWCNT is about 0.04 Å shorter than the corresponding Li−C distance in the pure SWCNT, and when Li is absorbed at outer sites, the Li−B distance is about 0.07 Å shorter than the corresponding Li−C distance in the pure SWCNT. In the case of the B_{C3}-doped SWCNT, the above corresponding values are 0.11 Å and 0.01 Å, respectively. As a result, there should be stronger interaction between B and Li. According to the calculation results, when Li atom is absorbed

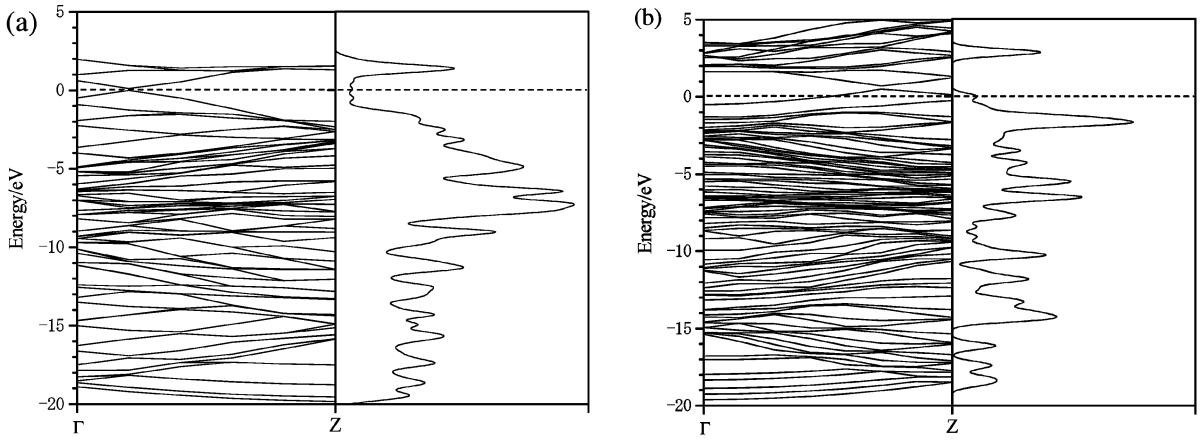

Figure 2. Calculated GGA band structures (left panel) and DOS (right panel) in pure (5, 5) SWCNT (a) and B-doped (5, 5) SWCNT (b). Here the doped B atom is substituted for the C1 atom. The dotted lines indicate Fermi levels.

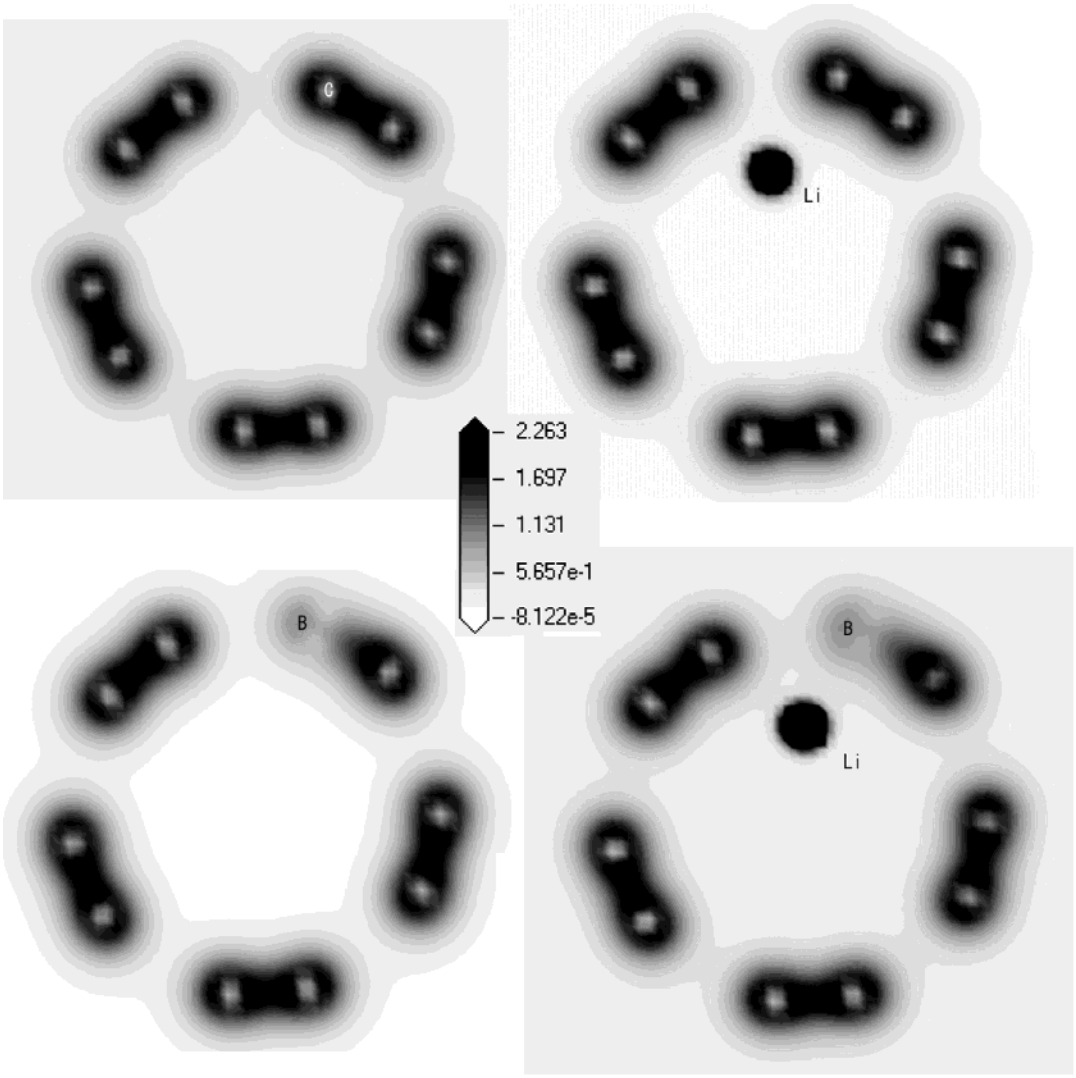

Figure 3. Charge density contour plots on a plane indicated as a dashed line S in Figure 1. Here the doped B atom is substituted for the C1 atom.

TABLE 2: Bond Length between C and B Atoms and Distance (Å) between the Absorbed Li and Neighboring Atoms Shown in Figure 1

	pure SWCNT	B_{C1}-doped SWCNT	B_{C3}-doped SWCNT	Li-absorbed SWCNT (inner)	Li-absorbed SWCNT (outer)	Li-absorbed B_{C1}−SWCNT (inner)	Li-absorbed B_{C1}−SWCNT (outer)	Li-absorbed B_{C3}−SWCNT (inner)	Li-absorbed B_{C3}−SWCNT (outer)
C1 −C2	1.410	1.474	1.391	1.419	1.416	1.478	1.473	1.403	1.396
C1−C3	1.412	1.474	1.471	1.418	1.417	1.478	1.474	1.473	1.466
C3−C4	1.411	1.404	1.494	1.416	1.429	1.417	1.425	1.506	1.512
C4−C5	1.412	1.423	1.403	1.418	1.417	1.425	1.424	1.410	1.410
C5−C6	1.410	1.422	1.418	1.419	1.417	1.424	1.423	1.427	1.425
C6−C2	1.411	1.404	1.433	1.418	1.428	1.418	1.424	1.441	1.451
Li−C1				2.146	2.343	2.105	2.276	2.068	2.376
Li−C2				2.229	2.163	2.207	2.118	2.231	2.174
Li−C3				2.424	2.183	2.238	2.132	2.327	2.176
Li−C4				2.433	2.171	2.306	2.160	2.348	2.144
Li−C5				2.158	2.323	2.180	2.292	2.147	2.303
Li−C6				2.238	2.149	2.277	2.145	2.276	2.105

in the SWCNT, Li atom will be changed to a cation and the electron will be transferred from the absorbed Li to the SWCNT and the negative charges will mainly be distributed among the neighboring C atoms of the wall. The net charges of the absorbed Li do not change apparently at the same absorption sites for both the pure and the B-doped SWCNT. However, the net charges of B change very significantly after the Li absorption, as shown in Table 3. The positive net charges of B decrease greatly after the Li absorption, indicating that the electron-deficient structure due to the B doping can effectively

TABLE 3: Net Charges of B in Different SWCNT

	B_{C1}	B_{C3}
B−SWCNT	+0.60	+0.60
Li^i−B−SWCNT	+0.22	+0.30
Li^0−B−SWCNT	+0.32	+0.23

accept the electrons from the absorbed Li atoms. Also it can be seen from Table 2 that, for the Li-absorbed SWCNT, the average C−C bond length increases by 0.5% (inner) and 0.71% (outer), respectively. For the B_{C1}-doped SWCNT, the average B/C−C

bond length increases by 0.45 (inner) and 0.52% (outer), respectively. And for the B_{C3}-doped SWCNT, the average B/C−C bond length increases by 0.56% (both inner and outer). These results mean that the strength of C−C covalent bonding decreases more significantly in the pure SWCNT than that of B/C−C covalent bonding in the B-doped SWCNT upon Li absorption. It is the usual case that the C−C covalent bonds are stretched and weakened due to Li absorption,[20] but the B-doping would weaken such effects, resulting from the fact that the doped B atoms accept more electrons transferred from the absorbed Li. Therefore, in addition to the Li−B ionic bonding is strengthened in the B-doped SWCNT, the effects of B-doping on the C/B−C covalent bonding should be another reason for the stronger binding in the B-doped SWCNT after Li absorption. In general, the above effects due to the B-doping can stabilize the C 6MRs and the absorbed Li, resulting in the stable chemical absorption of Li at these sites, so the Li absorption energies change to large negative values due to the B doping.

3.3. Formation Energies of B Impurity in SWCNT. When a B atom is substituted for a carbon atom in SWCNT, the formation energies are calculated to be about −0.01 eV whether the B atom is at the C1 or the C3 site, and the optimized structures exhibit that only the local structure around the doped B atom changes slightly. So it is easy to understand that the B-doped SWCNT has been prepared under rather mild conditions in many reports.[21−28]

The B substitutions in other graphitic carbon materials were deeply studied experimentally and theoretically.[29−32] However, the Li absorption in the B-doped SWCNT has not been paid enough attention to until now. Mukhopadhyay et al.[33] investigated the electrochemical Li insertion in the B-doped multiwalled carbon nanotubes (MWCNT). Though the B-doping effects were not dramatic, they really found that the B-doped MWCNT increased the Li insertion capacities due to their higher specific surface area, better 3D ordering, larger defect concentration, and higher conductivity. However, the tube-length increase was also found due to the B doping, which is regarded to have negative effects on the entry of Li into the tubes. It is worth expecting that the B-doping effects on Li absorption capability would be much more apparent in short SWCNT systems. The introduction of B into SWCNT should further be investigated, especially the B-doping effects on kinetic behavior of the entry and diffusion of Li.

4. Conclusion

In summary, according to the first-principles calculations results, the lithium absorption energies in the B-doped SWCNT are large negative values, compared with those in the pure SWCNT, whether Li is absorbed at inner sites or at outer sites of the tube walls. The B doping forms an electron-deficient structure in SWCNT, which can effectively accept the electrons from Li and stabilize the Li absorption on the tube wall. The calculation results suggest that enhanced Li absorption capability in the B-doped SWCNT should be expected.

Acknowledgment. The authors acknowledge the staffs at the Computer Center, Institute for Molecular Science, Okazaki National Institute for the use of the supercomputer. This study was supported by a Grant-in-Aid for Scientific Research from the Ministry of Education, Culture, Sports, Science and Technology of Japan and also by the 973 Program (2002CB211800) of China.

References and Notes

(1) Dillon, A. C.; Jones, K. M.; Bekkedahl, T. A.; Kiang, C. H.; Bethuune, D. S.; Heben, M. J. *Nature* **1997**, *386*, 377.

(2) Qin, X.; Gao, X. P.; Liu, H.; Yuan, H. T.; Yan, D. Y.; Gong, W. L.; Song, D. Y. *Electrochem. Solid-State Lett.* **2000**, *3* (12), 532.

(3) Che, G.; Lakshmi, B. B.; Fisher, E. R.; Martin, C. R. *Nature* **1998**, *393*, 346.

(4) Garau, C.; Frontera, A.; Quinonero, D.; Costa, A.; Ballester, P.; Deya, P. M. *Chem. Phys. Lett.* **2003**, *374* (5−6), 548.

(5) Wang, Q.; Chen, L. Q.; Huang X. J. *Electrochem. Solid-State Lett.* **2002**, *5* (9), A188−A190.

(6) Shimoda, H.; Gao, B.; Tang, X. P.; Kleinhammes, A.; Fleming, L.; Wu, Y.; Zhou, O. *Phys. Rev. Lett*. **2002**, *88* (1), 015502.

(7) Kar, T.; Pattanayak, J.; Scheiner, S. *J. Phys. Chem. A.* **2001**, *105* (45), 10397.

(8) Dahn, J. R.; Zheng, T.; Liu, Y.; Xue, J. S. *Science* **1995**, *270*, 590.

(9) Maurin, G.; Bousquet, Ch.; Henn, F.; Bernier, P.; Almairac, R.; Simon, B. *Chem. Phys. Lett.* **1999**, *312*, 14.

(10) Gao, B.; Kleinhammes, A.; Tang, X. P.; Bower, C.; Fleming, L.; Wu, Y.; Zhou, O. *Chem. Phys. Lett*. **1999**, *307*, 153.

(11) Claye, A. S.; Fischer, J. E.; Huffmann, C. B.; Rinzler, A. G.; Smalley, R. E. *J. Electrochem. Soc*. **2000**, *147*, 2845.

(12) Meunier, V.; Kephart, J.; Roland, C.; Bernholc, J. *Phys. Rew. Lett.* **2002**, *88* (7), 075506-1.

(13) Ceder, G.; Chiang, Y.-M.; Sadoway, D. R.; Aydinol, M. K.; Jang, Y.-I.; Huang, B. *Nature* **1998**, *392*, 694.

(14) Perdew, P.; Burke, K.; Wang, Y. *Phys. Rev. B* **1996**, *54*, 16533.

(15) Milman, V.; Winkler, B.; White, J. A.; Pickard, C. J.; Payne, M. C.; Akhmatskaya, E. V.; Nobes, R. H. *Int. J. Quantum Chem*. **2000**, *77*, 895.

(16) Vanderbilt, D. *Phys. Rev. B* **1990**, *41*, 7892.

(17) Dag, S.; Gulseren, O.; Yildirim, T.; Ciraci, S. *Phys. Rev. B* **2003**, *67*, 165424−1.

(18) Avdeev, V. V.; Savchenkova, A. P.; Monyakina, L. A.; Nikolskaya, I. V.; Khvostov, A. V. *J. Phys. Chem. Solids* **1996**, *57* (6−8), 947.

(19) Kganyago, K. R.; Ngoepe, P. E.; Catlow, C. R. A. *Solid State Ionics* **2003**, *159*, 21.

(20) Liu, Y.; Yukawa, H.; Morinaga, M. *Adv. Quantum Chem*. **2003**, *42*, 315.

(21) Han, W.; Bando, Y.; Kurashima, K.; Sato T. *Chem. Phys. Lett*. **1999**, *299*, 368.

(22) Satishkumar, B. C.; Govindraj, A.; Harikumar, K. R.; Zhang, J. P.; Cheetam, A. K.; Rao, C. N. R. *Chem. Phys. Lett.* **1999**, *300*, 473.

(23) Redlich, Ph.; Loeffler, J.; Ajayan, P. M.; Bill, J.; Aldinger, F.; Rühle, M. *Chem. Phys. Lett*. **1996**, *260*, 465.

(24) Han, W.; Bando, Y.; Kurashima, K.; Sato, T. *Appl. Phys. Lett.* **1998**, *73*, 3085.

(25) Golberg, D.; Bando, Y.; Kurashima, K.; Sato, T. *Chem. Phys. Lett*. **2000**, *323*, 185.

(26) Golberg, D.; Bando, Y.; Bourgeois, L.; Kurashima, K.; Sato, T. *Carbon* **2000**, *38*, 2017.

(27) Borowiak-Palen, E.; Pichler, T.; Fuentes, G. G.; Gra, A.; Kalenczuk, R. J.; Knupfer, M.; Fink, J. *Chem. Phys. Lett.* **2003**, *378*, 516.

(28) Golberg, D.; Bando, Y.; Han, W.; Kurashima, K.; Sato, T. *Chem. Phys. Lett*. **1999**, *308*, 337.

(29) Way, B. M.; Dahn, J. R. *J. Electrochem. Soc*. **1994**, *141*, 907.

(30) Weydanz W. J.; Way, B. M.; Buuren, T. V.; Dahn, J. R. *J. Electrochem. Soc*. **1994**, *141*, 900.

(31) Morita, M.; Hanada, T.; Tsutsumi, H.; Matsuda, Y.; Kawaguchi, M. *J. Electrochem. Soc*. **1992**, *139*, 1227.

(32) Kurita, N. *Carbon* **2000**, *38*, 65.

(33) Mukhopadhyay, I.; Hoshino, N.; Kawasaki, S.; Okino, F.; Hsu, W. K.; Touhara, H. *J. Electrochem. Soc.* **2002**, *49* (1), A39.